

Amorphous Host Materials Based on Tröger's Base Scaffold for Application in Phosphorescent Organic Light-Emitting Diodes

Ishita Neogi,[†] Samik Jhulki,[†] Avijit Ghosh,[‡] Tahsin J. Chow,^{*,‡} and Jarugu Narasimha Moorthy^{*,†}

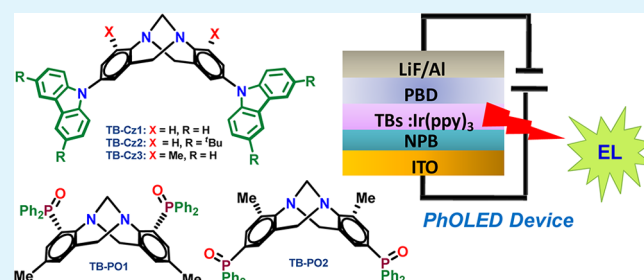
[†]Department of Chemistry, Indian Institute of Technology, Kanpur 208016, India

[‡]Institute of Chemistry, Academia Sinica, Taipei, Taiwan 115, Republic of China

Supporting Information

ABSTRACT: Tröger's bases (TBs) functionalized with carbazoles (TB-Czs) and phosphine oxides (TB-POs) were designed and synthesized as host materials for application in phosphorescent organic light-emitting diodes. The TB scaffold is shown to impart thermal stability with high T_g values (171–211 °C) as well as high triplet energies in the range of 2.9–3.0 eV. With a limited experimentation of the devices, it is shown that the TBs doped with a green phosphor, namely, Ir(ppy)₃, permit impressive external efficiencies on the order of ca. 16% with a high brightness of ca. 3000–4000 cd/m². Better device performance results are demonstrated by a small structural manipulation of the TB scaffold involving substitution of methyl groups in the core scaffold.

KEYWORDS: Tröger's base, host materials, phosphor, phosphorescence, triplet energy, pholeds



INTRODUCTION

Research on organic light-emitting diodes (OLEDs) continues to be an exciting enterprise, which is most relevant commercially from the point of view of lighting and display technology. The advantages that OLED-based displays and lighting offer are unmatched by other existing technologies. Thus, the motivation to develop novel functional materials with improved performance of fabricated devices continues unabated.^{1–8} Over the past decade, there has been a gradual shift of interest from fluorescence- to phosphorescence-based materials in quest of high efficiencies of light emission by harvesting both singlet and triplet excitons.^{9–12} It is now firmly established that the organometallic complexes of certain heavy metals such as Ir, Os, Pt, etc. may allow 100% internal quantum efficiency by means of facile spin–orbit coupling.¹³ However, an inevitable shortcoming associated with such phosphorescence-emitting materials in nondoped devices is the quenching due to concentration and triplet–triplet annihilation.¹⁴ These detrimental nonradiative decay mechanisms can be suppressed by dispersing triplet phosphors in a host matrix.^{15,16} The design and development of host materials suitable for a certain emitter continue to be a challenge, as the following criteria must be met for a material to be considered as a suitable host for a given guest:^{17–19} first, the host material should possess higher triplet energy than the triplet phosphor to prevent reverse energy transfer from the latter back to the host; second, the highest occupied molecular orbital (HOMO) and lowest unoccupied molecular orbital (LUMO) energies of the host material should be such that the holes and electrons can be injected in a facile manner from adjacent layers; third,

the compounds should be thermally and morphologically stable.

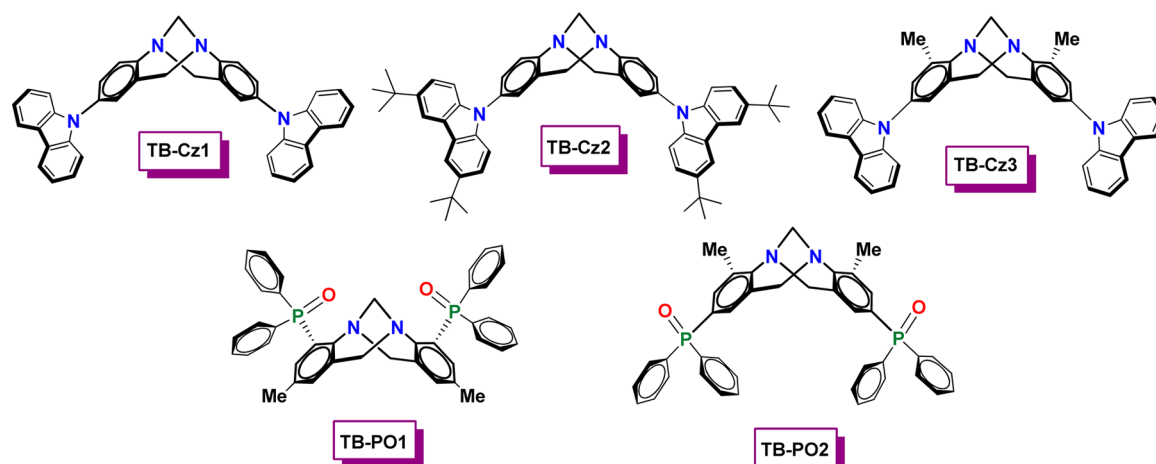
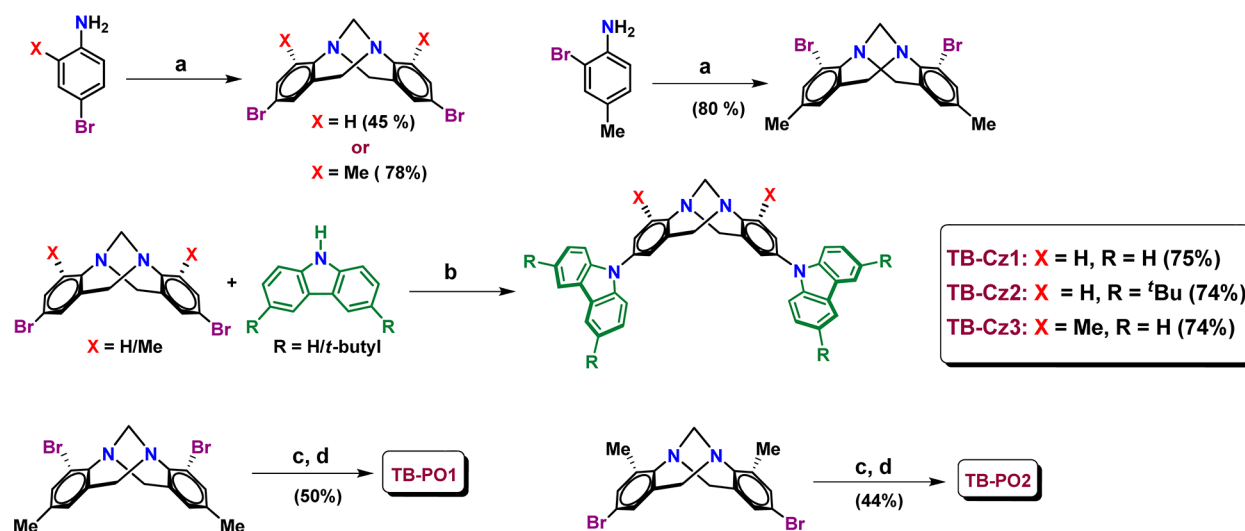
The conventional host materials, namely, *m*CP(1,3-bis(*N*-carbazolyl)benzene)²⁰ and CBP (4,4'-bis(*N*-carbazolyl)-1,1'-biphenyl),²¹ suffer from the disadvantage of low glass-transition temperatures (T_g values), which are 60 and 62 °C, respectively. In continuation of our studies based on the *de novo* design of organic materials for application in OLEDs,^{22–26} we surmised that Tröger's Base (TB) scaffold, which is V-shaped, rigid, chiral, and C_2 -symmetric,²⁷ can be exploited to impart amorphous property and develop host materials with high T_g values for phosphorescent OLEDs (PhOLEDs). This is based on the knowledge from a just-concluded study in our group that the TB scaffold does indeed render the 2,8-substituted derivatives highly amorphous and thermally stable.²⁸ Accordingly, we designed carbazole- and phosphine oxide-functionalized TBs, that is, TB-Cz1–3 and TB-PO1–2 in Chart 1, for application as host materials; the functionalities such as carbazole and phosphine oxide appended to the TB scaffold have been proven to be excellent for high triplet energy in phosphorescent OLEDs.^{29–35} Herein, we report the synthesis, photophysical, electrochemical, and thermal studies of TBs functionalized with carbazoles (TB-Czs) and phosphine oxides (TB-POs, Chart 1) and demonstrate the applicability of these materials as host materials in simple PhOLED devices for green emission from the dopant, that is, Ir(ppy)₃.

Received: November 19, 2014

Accepted: January 13, 2015

Published: January 13, 2015

Chart 1. Structures of TBs Functionalized with Carbazole and Phosphine Oxide

Scheme 1. Synthesis of TB-Czs and TB-POs^a

^aReagents and conditions: (a) $(\text{HCHO})_n$, TFA, -20°C , 48 h; (b) $\text{Pd}(\text{OAc})_2$, $\text{P}(t\text{Bu})_3$, NaO^tBu , dry toluene, 110°C , 72 h; (c) $n\text{BuLi}$, THF, -78°C , Ph_2PCl , 12 h; (d) H_2O_2 , 0°C , 30 min.

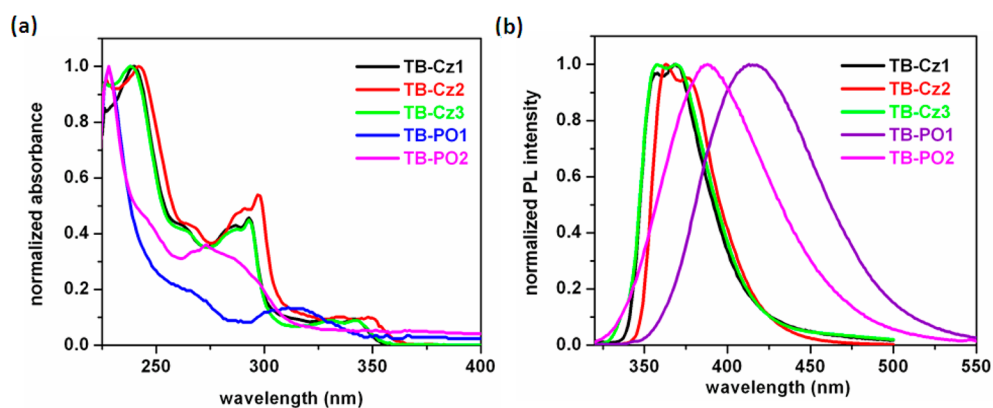


Figure 1. (a) Normalized absorption and (b) emission spectra of TBs in dilute DCM solutions.

RESULTS AND DISCUSSION

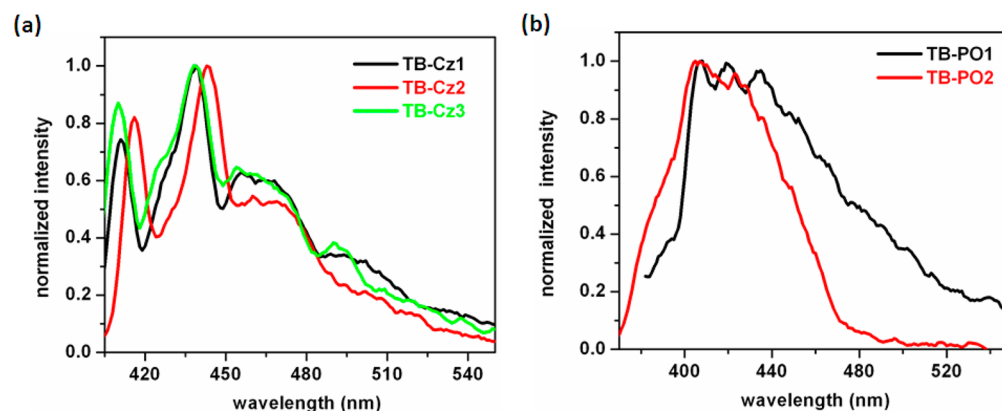
Synthesis. The 2,8-dibromo-substituted TBs, that is, 2,8-dibromo-6H,12H-5,11-methanodibenzo[*b,f*][1,5]-diazocine, 2,8-dibromo-4,10-dimethyl-6H,12H-5,11-methanodibenzo[*b,f*][1,5]-diazocine and 4,10-dibromo-2,8-dimethyl-6H,12H-

5,11-methanodibenzo[*b,f*][1,5]-diazocine, were synthesized by following the literature-reported procedures.^{36–38} 2-Fold Buchwald-Hartwig amination of these bromo-substituted TBs with carbazole or 3,6-di-*tert*-butylcarbazole afforded three carbazole functionalized TBs, that is, TB-Cz1, TB-Cz2 and

Table 1. Absorption, Fluorescence, Phosphorescence, Electrochemical, and Thermal Properties of TB-Cz1–3, TB-PO1, and TB-PO2

substrate	λ_{\max} (UV) ^a (nm)	band gap ^b (eV)	λ_{\max} (PL) sol ^a (nm)	HOMO/LUMO (eV)	E_T (eV) ^c	T_d ^d	T_g ^e
TB-Cz1	240	3.50	368	5.38/1.88	3.03	394	171
TB-Cz2	242	3.42	363	5.44/2.02	2.99	424	211
TB-Cz3	240	3.51	369	5.54/2.03	3.03	405	175
TB-PO1	228	3.60	413	5.42/1.82	3.07	384	196
TB-PO2	228	3.98	388	5.56/1.58	3.0	404	200

^aAbsorption and fluorescence spectra were recorded in DCM solutions (ca. 1×10^{-5} M). ^bBand-gap energies were calculated from red edge absorption onset values. ^cThe E_T values were calculated from highest energy peak of phosphorescent spectra recorded in 2-methyltetrahydrofuran at 77 K. ^dFrom TGA corresponding to 5% weight loss. ^eFrom DSC.

**Figure 2.** Phosphorescence spectra of TB-Czs (a) and TB-POs (b) in 2-methyltetrahydrofuran (1×10^{-5} M) at 77 K.

TB-Cz3, in ca. 74–75% isolated yield (Scheme 1). Syntheses of the phosphine oxides involved lithiation of their respective dibromo-TBs at low temperature followed by quenching with chlorodiphenylphosphine to yield corresponding phosphines. The latter were subjected to oxidation using H_2O_2 at ambient temperature. The two-step synthesis afforded TB-PO1 and TB-PO2 in 44–50% isolated yields (cf. Scheme 1).

Photophysical Properties. UV–vis absorption spectra of all TBs were recorded with dilute dichloromethane (DCM) solutions (ca. 1×10^{-5} M). As shown in Figure 1, one observes structured absorption for TB-Cz1, TB-Cz2, and TB-Cz3 with the absorption for TB-Cz2 slightly red-shifted. In contrast, the absorption spectra of both phosphine oxides, that is, TB-PO1 and TB-PO2, are quite different and display primarily two absorption maxima. Although the absorption maximum in the short wavelength region for both TB-PO1 and TB-PO2 lies at the same position (ca. 230 nm), the long-wavelength absorption is shifted bathochromically by ~ 40 nm for TB-PO1 when compared to that of TB-PO2. Band gaps of all the TBs were calculated from their absorption onset values. Phosphine oxide-functionalized TBs, that is, TB-POs, exhibited comparatively higher band gap energies than their carbazole counterparts (cf. Table 1). In particular, it is noteworthy that the band gap for 2,8-functionalized phosphine oxide, that is, TB-PO2, is higher than that for the 4,10 isomer, that is, TB-PO1.

Fluorescence spectra of all TBs were recorded with dilute DCM solutions (ca. 1×10^{-6} M) for excitation at 300 nm except for TB-PO2; for the latter, the fluorescence spectrum was recorded for excitation at 273 nm. Photoluminescence spectral features of all carbazole derivatives, that is, TB-Czs, are similar with emission maximum at ca. 363–369 nm; note that the band with emission maximum is closely spaced by another strong emission band within ca. 10–15 nm. Emission maxima

for TB-POs are quite broad and are bathochromically shifted relative to those of TB-Czs. It is noteworthy that the emission maximum of TB-PO1 is, in particular, red-shifted by ~ 25 nm relative to that of TB-PO2, which is quite intriguing. One would expect, based on steric inhibition of resonance at *o*-position, that the absorption as well as emission maxima should be red-shifted for the para isomer, that is, TB-PO2, relative to the ortho one, that is, TB-PO1. Presumably, nitrogen lone pair delocalization into the ring occurs more efficiently in TB-PO1 due to the assistance by the proximate oxygen of phosphine oxide to account for the observed red shift in the emission as well as absorption maxima of TB-PO1; we believe that the oxygen atom of phosphine oxide and nitrogen atom of the TB core that undergoes charge delocalization interact effectively.

Triplet energies of all the TBs were derived from 0 to 0 transitions in the phosphorescence spectra recorded in dilute 2-methyltetrahydrofuran solution (ca. 1×10^{-6} M) at 77 K (cf. Figure 2). All the compounds were found to possess high triplet energies in the range of 2.9–3.0 eV, which is higher than the triplet energy of the conventional green dopant, namely, Ir(ppy)₃ (2.42 eV).³⁹

Electrochemical Properties. Electrochemical properties of the TBs were investigated by cyclic voltammetry. All the TB-substituted carbazoles, that is, TB-Czs, exhibited irreversible oxidation in DCM solutions (ca. 1×10^{-3} M) on anodic sweep (cf. Supporting Information). Phosphine oxides, that is, TB-POs, exhibited irreversible oxidations similar to carbazole analogues on anodic sweeping of their DCM solutions. The peak corresponding to reduction wave was prominent in case of TB-PO2. However, it was not conspicuous for TB-PO1. The HOMO energies were calculated from onset oxidation potentials using the equation $HOMO = -e(E_{\text{onset(ox)}} - E_{1/2, Fc/Fc+}) - 4.8$ eV. The energies of LUMOs were obtained

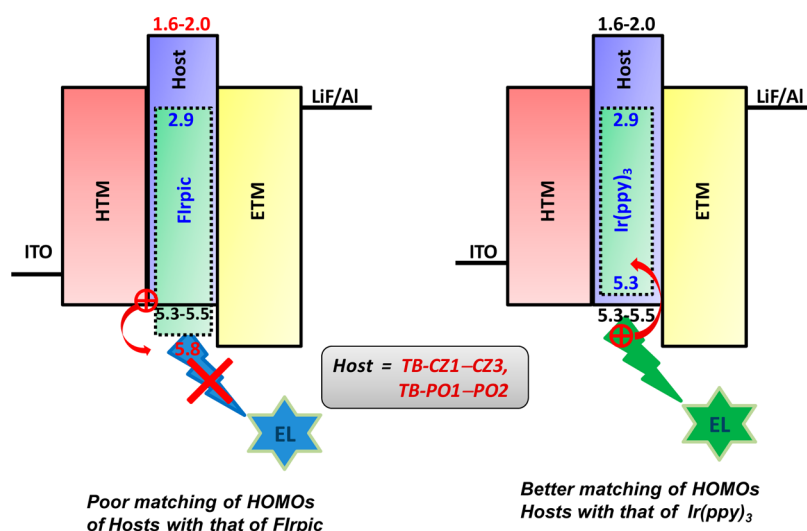


Figure 3. Relative energy-level diagrams of TB-based PhOLED devices with Irpic (left) and Ir(ppy)₃ (right) as phosphors.

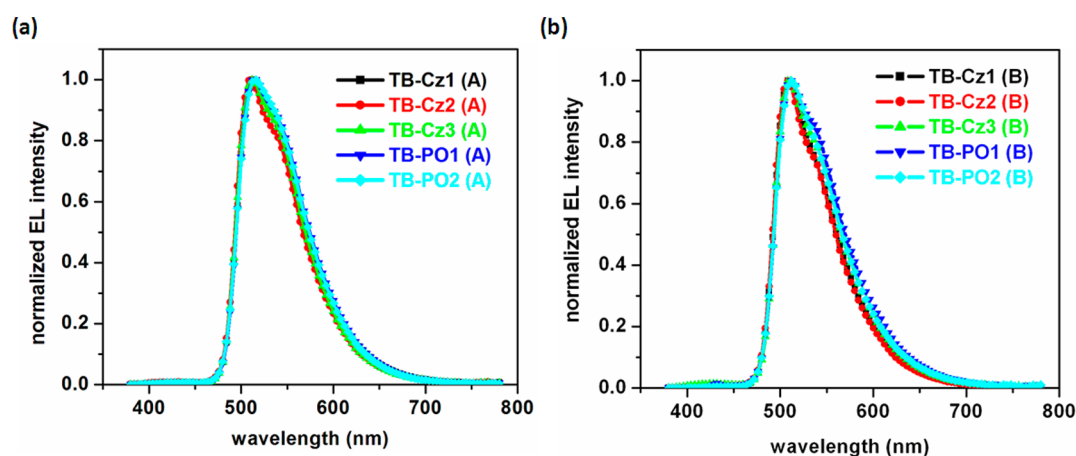


Figure 4. EL spectra recorded from the devices of TBs with configuration A (a) and B (b).

by subtracting the band-gap energies from their corresponding HOMO levels.

Thermal Properties. Thermal properties of the TBs were examined by thermogravimetric (TGA) and differential scanning calorimetric (DSC) analysis at a heating rate of 10 °C/min under inert atmosphere. Indeed, all compounds exhibited very high thermal decomposition and T_g values (Table 1), which indicates their ability to endure high thermal stress during vacuum sublimation and joule heating. The excellent thermal properties of TB-based materials may be ascribed to the rigidity of the core scaffold and its unique V-shaped geometry, which prevents molecular aggregation leading to stable glass formation. Among carbazole-functionalized TBs, the bulky *tert*-butyl groups in TB-Cz2 contribute to its significantly high thermal stability. The amorphous property of all carbazole-functionalized TBs (Chart 1) was additionally confirmed by featureless and broad powder X-ray diffraction patterns (cf. Supporting Information). Unfortunately, phosphine oxide derivatives TB-POs were found to exhibit microcrystallinity in the solid state as revealed by their X-ray diffraction patterns.

Electroluminescent Properties. As mentioned earlier, the triplet energies of all the synthesized TB-based hosts fall in the range of ca. 2.9–3.0 eV, which is higher than that of blue emissive dopant, that is, Irpic ($E_T = 2.65$ eV).⁴⁰ Thus, our

initial efforts were focused on examining their applicability for Irpic as the dopant in PhOLED devices for blue emission. Unfortunately, the results of device performances were disappointing (cf. Supporting Information). Inefficient energy transfer from the hosts to the guests was believed to be the reason for poor efficiency as well as the observed mixed emission emanating from the dopant as well as the host. A careful analysis of the relative energy levels of all materials employed in the devices led us to infer two major impediments for the observed poor results for the devices constructed with Irpic as the phosphor: first, the LUMO levels of the hosts are very high in energy due to e-rich TB scaffold, which presumably decelerates transport of electrons from the electron-transporting TmPyPB layer to the host material, Figure 3. Consequently, population of the electrons injected into the emissive layer is presumably incommensurate to the high population of holes that are accumulated; second, the HOMO levels of the host Irpic are higher in energy than those of TBs, which not only hinders hole transport from the host to Irpic leading to poor efficiency but also causes accumulation of holes in the host material. Inefficient energy transfer due to incommensurate HOMO–LUMO levels may result in emission from the host itself in addition to concentration quenching (cf. Supporting Information). We therefore surmised that replacement of TmPyPB with a relatively higher LUMO electron-

Table 2. Device Performance Results for PhOLED Devices Fabricated with TBs as Host Materials

compound	device	V_{on}^a	η_{ext}^b	η_p^c	η_l^d	$\lambda_{max}^{EL}^e$	L_{max}^f	CIE (x,y) ^g
TB-Cz1	A	3.5	5.2	10.2	18.1	512	9820	0.31, 0.60
	B	4.5	6.3	9.0	21.0	508	2770	0.29, 0.60
TB-Cz2	A	4.5	4.9	8.02	16.6	512	1450	0.30, 0.60
	B	5.5	15	42.3	24.1	508	312	0.29, 0.59
TB-Cz3	A	4.0	16.0	34.6	54.8	512	4020	0.30, 0.61
	B	4.5	7.40	16.1	23.1	512	2828	0.30, 0.60
TB-PO1	A	4.0	6.9	17.1	23.5	516	2752	0.31, 0.60
	B	4.5	2.7	3.3	8.9	512	359	0.31, 0.58
TB-PO2	A	3.0	8.3	23.8	28.6	516	2860	0.31, 0.60
	B	3.5	7.0	15.6	17.4	512	3100	0.30, 0.60

^aTurn-on voltage (V). ^bMaximum external quantum efficiency (%). ^cMaximum power efficiency (lm/W). ^dMaximum luminance efficiency (cd/A). ^e λ_{max}^{EL} (nm). ^fMaximum luminance achieved (cd/m²). ^g1931 chromaticity coordinates.

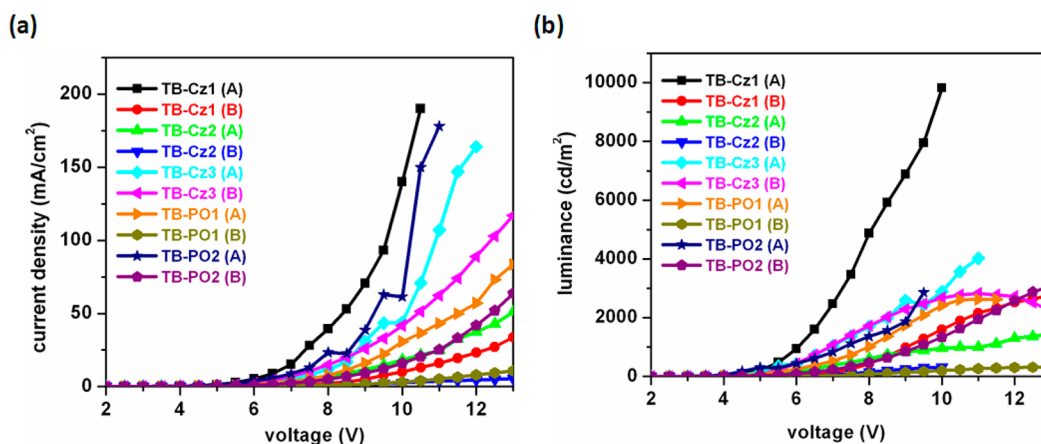


Figure 5. Current density vs voltage (a) and luminance vs voltage (b) profiles for the PhOLED devices constructed for TB-based host materials with configurations A and B.

transporting material such as 2-(4-*tert*-butylphenyl)-5-(4-biphenyl)-1,3,4-oxadiazole (PBD) and that of Firpic with a dopant possessing relatively higher HOMO such as Ir(ppy)₃ might improve the device results; note that the LUMO and HOMO for PBD and Ir(ppy)₃ are 2.4¹² and 5.3 eV,⁴¹ respectively. Accordingly, two devices of the following configurations were fabricated: configuration A = ITO/NPB (40 nm)/TB-Czs or TB-POs: Ir(ppy)₃(8–9%, 30 nm)/PBD (40 nm)/LiF (2 nm)/Al (150 nm) and configuration B = ITO/NPB (40 nm)/TCTA (10 nm)/TB-Czs or TB-POs: Ir(ppy)₃(8–9%, 30 nm)/TPBI (40 nm)/LiF (2 nm)/Al (150 nm), where ITO functions as anode, NPB and/or TCTA function as hole-transporting materials, PBD and/or TPBI function as electron-transporting as well as hole-blocking materials, and LiF/Al serves as a composite cathode. Of course, the emissive layer was constructed by coevaporation of TB-based host and green-emissive dopant, namely, Ir(ppy)₃. Bright green electroluminescence that is characteristic of Ir(ppy)₃ was captured from all the devices. Most remarkably, no emission from the host was observed from any of the devices (cf. Figure 4). The results of electroluminescence captured from the two devices for all TBs are collected in Table 2, and the corresponding *I*–*V*–*L* characteristics of the devices are shown in Figure 5.

As may be perused from Table 2, all TB-based host materials function as hosts for the green emissive phosphor, that is, Ir(ppy)₃. Among the carbazole-based derivatives, the performance with TB-Cz3 is most impressive, followed by that of TB-Cz1 and TB-Cz2. In fact, maximum external quantum efficiency of 16.0%, maximum luminous efficiency of 54.8 cd/

A, and maximum power efficiency of 34.6 lm/W were obtained for TB-Cz3 as the host material in the device configuration A. Although the efficiency parameters for TB-Cz2 host in the device configuration B are higher, it is noteworthy that the efficiency roll-off is very high, and the maximum brightness is limited to 312 cd/m². In fact, the poorer performance exhibited by TB-Cz2 when compared to other two carbazole derivatives may be a consequence of appended bulky tertiary butyl groups, which appear to function effectively functioning as electrical insulating entities thereby constraining charge transport.⁴² The reason why one observes better device performance results with TB-Cz3 as the host material should be traceable to the influence of the methyl group, which seemingly facilitates better energy transfer; presumably, the host accommodates the dopant in close proximities where the energy transfer is more efficient.

Insofar as the TB-based phosphine oxides are concerned, the performance exhibited by TB-PO2 as the host material is far better than that of its structural isomer TB-PO1. A careful analysis of their energy levels (Figure 3) reveals that TB-PO1 has a higher HOMO level and a low-lying LUMO level when compared to that of TB-PO2. Presumably, electron injection is facile in the case of TB-PO1, but hole migration from host to dopant is easier in the case of TB-PO2. This is further corroborated by the poor device performances noted for Firpic as the dopant, for which the HOMO energy is much deeper. Thus, it emerges that the substitution of methyl groups in the TB skeleton leads to a subtle lowering of the HOMO levels by

ca. 0.16 eV (TB-Cz1 vs TB-Cz3), which manifests in dramatic improvement of the device performance results.

CONCLUSIONS

Two distinct sets of host materials based on the TB scaffold, namely, carbazoles and phosphine oxides, have been designed and synthesized; it is noteworthy that the simple synthetic protocol allows a ready access to these materials. The TB scaffold is found to impart amorphous property to all the carbazole and phosphine oxide derivatives with high T_g values, which range from 171 to 211 °C. Although all TBs were found to possess large band-gap energy of ca. 2.9–3.0 V, their utility for application as host materials for blue phosphor, that is, FIrPic, was curtailed by poor device performance results. Otherwise, the fact that they function as remarkable host materials for green-emissive Ir(ppy)₃ is demonstrated by impressive device performance results. With a limited experimentation with device constructions, external efficiencies on the order of ca. 16% with a high brightness of ca. 3000–4000 cd/m² have been observed for both carbazole- and phosphine oxide-functionalized TB hosts. It is shown that structural manipulation of the TB scaffold by substitution of methyl groups in the core scaffold allows better performance results of the devices when employed as host materials. Thus, utility of the readily accessible V-shaped Tröger's bases, which are known for well over a century and have elicited considerable interest as chiral scaffolds in molecular recognition, is compellingly demonstrated for application in PhOLEDs.

EXPERIMENTAL SECTION

Synthesis of TB-Cz1. An oven-dried pressure tube was cooled under nitrogen gas and charged with 2,8-dibromo-6*H*,12*H*-5,11-methanodi-benzo[*b,f*][1,5]-diazocine (0.50 g, 1.31 mmol), carbazole (0.57 g, 3.42 mmol), NaO^tBu (0.60 g, 5.26 mmol), Pd(OAc)₂ (0.03 g, 10 mol %), and P^t(Bu)₃ (32 μL, 0.13 mmol). To the contents was added 10 mL of dry toluene. The pressure tube was sealed under nitrogen and heated at 100 °C for 72 h. After this period, the contents were cooled to room temperature, toluene was removed in vacuo, and the reaction mixture was quenched with water. The organic contents were extracted with chloroform, and the combined extract was dried over anhydrous (anhyd) Na₂SO₄ and filtered. The solvent was removed in vacuo, and the crude product was subjected to neutral alumina column chromatography using ethyl acetate/petroleum ether (20:80) as an eluent to yield pure TB-Cz1 as a colorless solid material, 0.72 g (75% yield); IR (solid) cm⁻¹ 3044, 2944, 1595, 1495, 1451, 1334, 1323, 1308, 1229, 1207; ¹H NMR (CDCl₃, 500 MHz) δ 4.35 (d, *J* = 16.5 Hz, 2H), 4.48 (s, 2H), 4.87 (d, *J* = 16.5 Hz, 2H), 7.20–7.25 (m, 6H), 7.37–7.40 (m, 12H), 8.11 (d, *J* = 7.35 Hz, 4H); ¹³C NMR (CDCl₃, 125 MHz) δ 58.6, 66.9, 109.8, 120.0, 120.4, 123.3, 125.4, 126.0, 126.5, 126.7, 129.1, 133.8, 141.0, 146.8; electron impact mass spectrometry (EI-MS⁺) *m/z* Calcd for C₃₅H₂₉N₄ 553.2392 [M + H]⁺, found 552.2391.

Synthesis of TB-Cz2. A similar procedure to that described above for the synthesis of TB-Cz1 was adopted for the synthesis of TB-Cz2 by employing 2,8-dibromo-4,10-dimethyl-6*H*,12*H*-5,11-methanodi-benzo[*b,f*][1,5]-diazocine (0.50 g, 1.31 mmol) and 3,6-di-*tert*-butylcarbazole (0.96 g, 2.6 mmol). The solvent was removed in vacuo, and the crude product was subjected to neutral alumina column chromatography using ethyl acetate/petroleum ether (5:95) as an eluent to yield pure TB-Cz2 as a colorless powder (0.50 g, 74% yield); IR (film) cm⁻¹ 2958, 2865, 1492, 1363, 1262, 1294; ¹H NMR (CDCl₃, 500 MHz) δ 1.46 (s, 36H), 4.35 (d, *J* = 16.5 Hz, 2H), 4.50 (s, 2H), 4.87 (d, *J* = 16.5 Hz, 2H), 7.19 (s, 2H), 7.30–7.45 (m, 12H), 8.13 (s, 4H); ¹³C NMR (CDCl₃, 125 MHz) δ 31.9, 34.6, 58.5, 66.8, 109.1,

116.1, 123.2, 123.5, 124.9, 126.1, 126.4, 128.8, 134.4, 139.2, 142.8; EI-MS⁺ *m/z* Calcd for C₃₅H₄₁N₄ 777.4896 [M + H]⁺, found 777.4891.

Synthesis of TB-Cz3. A similar procedure to that described above for the synthesis of TB-Cz1 was followed for the synthesis of TB-Cz3 by employing 2,8-dibromo-4,10-dimethyl-6*H*,12*H*-5,11-methanodi-benzo[*b,f*][1,5]-diazocine (0.50 g, 1.22 mmol) and carbazole (0.47 g, 2.3 mmol). The workup followed by neutral alumina column chromatography using ethyl acetate/petroleum ether (10:90) as an eluent led to yield pure TB-Cz3 as a white powder (0.50 g, 74% yield); IR (KBr) cm⁻¹ 3048, 2947, 1597, 1493, 1477, 1452, 1311, 1230, 1209; ¹H NMR (CDCl₃, 500 MHz) δ 2.52 (s, 6H), 4.19 (d, *J* = 17.1 Hz, 2H), 4.49 (s, 2H), 4.77 (d, *J* = 17.1 Hz, 2H), 7.07 (s, 2H), 7.26–7.29 (m, 6H), 7.41 (brs, 8H), 8.14 (d, *J* = 8.0 Hz, 4H); ¹³C NMR (CDCl₃, 125 MHz) δ 17.2, 55.0, 67.5, 109.8, 119.7, 120.2, 122.8, 123.2, 125.8, 127.6, 129.5, 133.3, 135.0, 141.0, 145.3; electrospray ionization mass spectrometry (ESI-MS⁺) *m/z* Calcd for C₄₁H₃₃N₄ 581.2705 [M + H]⁺, found 581.2707.

Synthesis of TB-PO1. A solution of 4,10-dibromo-2,8-dimethyl-6*H*,12*H*-5,11-methanodi-benzo[*b,f*][1,5]-diazocine (1.0 g, 2.45 mmol) in 50 mL of anhydrous tetrahydrofuran (THF) was cooled to –78 °C under nitrogen gas atmosphere. To this solution was introduced *n*-butyllithium (7.0 mL, 9.8 mmol, 1.4 M in hexane) very slowly under N₂ atmosphere. The contents were allowed to stir at –78 °C for 1 h, and chlorodiphenylphosphine (2.2 mL, 12.2 mmol) was added slowly at –78 °C. The reaction mixture was observed to turn pale yellow and was allowed to warm to room temperature very slowly. The reaction mixture was further stirred for 16 h before the reaction was quenched with water. Subsequently, the reaction mixture was stripped off the THF in vacuo, and the organic contents were extracted with chloroform. The combined extract was dried over anhyd Na₂SO₄ and filtered, and the solvent was removed in vacuo.

The white material obtained from the above operation was dissolved in 25 mL of DCM at 0 °C. To the resultant solution was added 30% aqueous H₂O₂ (0.6 mL), and the solution was stirred for 20 min at room temperature. The reaction mixture was quenched with water, and the organic material was extracted with DCM. The combined extract was dried over anhyd Na₂SO₄ and filtered, and the solvent was removed in vacuo. The crude product was subjected to neutral alumina column chromatography using ethyl acetate/petroleum ether (50:50) as an eluent to yield pure TB-PO1 as a white powder (0.80 g, 50.3% overall yield); IR (film) cm⁻¹ 2963, 2917, 2849, 1435, 1260, 1097, 1020; ¹H NMR (CDCl₃, 500 MHz) δ 2.09 (s, 6H), 3.51 (s, 2H), 4.36 (d, *J* = 18.3 Hz, 2H), 4.72 (d, *J* = 18.3 Hz, 2H), 6.68 (d, *J* = 14.05 Hz, 2H), 6.93 (s, 2H), 7.35–7.57 (m, 16H), 7.66–7.70 (m, 4H); ¹³C NMR (CDCl₃, 125 MHz) δ 20.9, 57.8, 65.7, 126.9, 127.8, 127.9, 128.0, 128.1, 128.2, 130.70, 130.78, 131.3, 132.0, 132.2, 132.3, 132.8, 133.4, 133.5, 133.6, 134.5, 135.4; ³¹P NMR (CDCl₃, 500 MHz) δ 28.6; ESI-MS⁺ *m/z* Calcd for C₄₁H₃₇N₂O₂P₂ 651.2330 [M + H]⁺, found 651.2332.

Synthesis of TB-PO2. A procedure similar to the one described above for the synthesis of TB-PO1 was followed for the synthesis of TB-PO2 using 2,8-dibromo-4,10-dimethyl-6*H*,12*H*-5,11-methanodi-benzo[*b,f*][1,5]-diazocine (1.0 g, 2.45 mmol). After the reaction, the crude product was subjected to neutral alumina column chromatography using ethyl acetate/petroleum ether (80:20) as an eluent to yield pure TB-PO2 as a white powder (0.70 g, 44% overall yield); IR (film) cm⁻¹ 3055, 2953, 1590, 1468, 1437, 1178, 1113; ¹H NMR (CDCl₃, 500 MHz) δ 2.32 (s, 6H), 3.97 (d, *J* = 16.5 Hz, 2H), 4.28 (s, 2H), 4.54 (d, *J* = 16.5 Hz, 2H), 7.13 (d, *J* = 12.2 Hz, 2H), 7.22 (d, *J* = 12.2 Hz, 2H), 7.43–7.54 (m, 12H), 7.62–7.67 (m, 8H); ¹³C NMR (CDCl₃, 125 MHz) δ 17.2, 54.7, 67.1, 126.8, 127.6, 128.2, 128.3, 128.4, 128.5, 128.6, 131.8, 132.0, 132.1, 132.3, 132.4, 132.8, 133.4, 133.5, 149.6; ³¹P NMR (CDCl₃, 500 MHz) δ 29.5; ESI-MS⁺ *m/z* Calcd for C₄₁H₃₇N₂O₂P₂ 651.2330 [M + H]⁺, found 651.2339.

ASSOCIATED CONTENT

Supporting Information

Cyclic voltammograms, DSC and TGA profiles, EL spectra, associated plots for the devices constructed, and ¹H, ¹³C, and

³¹P NMR spectral reproductions of all the compounds reported. This material is available free of charge via the Internet at <http://pubs.acs.org>.

AUTHOR INFORMATION

Corresponding Authors

*E-mail: moorthy@iitk.ac.in. (J.N.M.)

*E-mail: tjchow@chem.sinica.edu.tw. (T.J.C.)

Notes

The authors declare no competing financial interest.

ACKNOWLEDGMENTS

J.N.M. is thankful to SERB, New Delhi, for generous financial support. I.N. and S.J. thank CSIR, New Delhi, for their senior research fellowships. We acknowledge the optoelectronic device fabrication and testing by the scientific instrument facility at the Institute of Chemistry, Academia Sinica, Taipei.

REFERENCES

- (1) Kraft, A.; Grimsdale, A. C.; Holmes, A. B. Electroluminescent Conjugated Polymers-Seeing Polymers in a New Light. *Angew. Chem., Int. Ed.* **1998**, *37*, 402–408.
- (2) Bernius, M. T.; Inbasekaran, M.; O'Brien, J.; Wu, W. Progress with Light-Emitting Polymers. *Adv. Mater.* **2000**, *12*, 1737–1750.
- (3) Shirota, Y. Organic Materials for Electronic and Optoelectronic Devices. *J. Mater. Chem.* **2000**, *10*, 1–25.
- (4) Hung, L. S.; Chen, C. H. Recent Progress of Molecular Organic Electroluminescent Materials and Devices. *Mater. Sci. Eng., R.* **2002**, *39*, 143–222.
- (5) Kulkarni, A. P.; Tonzola, C. J.; Babel, A.; Jenekhe, S. A. Electron Transport Materials for Organic Light-Emitting Diodes. *Chem. Mater.* **2004**, *16*, 4556–4573.
- (6) Hughes, G.; Bryce, M. R. Electron-Transporting Materials for Organic Electroluminescent and Electrophosphorescent Devices. *J. Mater. Chem.* **2005**, *15*, 94–107.
- (7) Shirota, Y.; Kageyama, H. Charge Carrier Transporting Molecular Materials and Their Applications in Devices. *Chem. Rev.* **2007**, *107*, 953–1010.
- (8) Hwang, S.-H.; Moorefield, C. N.; Newcome, G. R. Dendritic Macromolecules for Organic Light-Emitting Diodes. *Chem. Soc. Rev.* **2008**, *37*, 2543–2557.
- (9) Baldo, M. A.; O'Brien, D. F.; You, Y.; Shoustikov, A.; Sibley, S.; Thompson, M. E.; Forrest, S. R. Highly Efficient Phosphorescent Emission from Organic Electroluminescent Devices. *Nature* **1998**, *395*, 151–154.
- (10) Baldo, M. A.; Lamansky, S. P.; Burrows, E.; Thompson, M. E.; Forrest, S. R. Very High-Efficiency Green Organic Light-Emitting Devices Based on Electrophosphorescence. *Appl. Phys. Lett.* **1999**, *75*, 4–6.
- (11) Sun, Y.; Giebink, N. C.; Kanno, H.; Ma, B.; Thompson, M. E.; Forrest, S. R. Management of Singlet and Triplet Excitons for Efficient White Organic Light-Emitting Devices. *Nature* **2006**, *440*, 908–912.
- (12) Tao, Y.; Yang, C.; Qin, J. Organic Host Materials for Phosphorescent Organic Light-Emitting Diodes. *Chem. Soc. Rev.* **2011**, *40*, 2943–2970.
- (13) Xu, H.; Chen, R.; Sun, Q.; Wenyong, L.; Su, Q.; Huang, W.; Liu, X. Recent Progress in Metal-Organic Complexes for Optoelectronic Applications. *Chem. Soc. Rev.* **2014**, *43*, 3259–3302.
- (14) Baldo, M. A.; Adachi, C.; Forrest, S. R. Transient Analysis of Triplet-Triplet Annihilation Transient Analysis of Organic Electrophosphorescence. *Phys. Rev. B: Condens. Matter Mater. Phys.* **2000**, *62*, 10967–10977.
- (15) Yeh, S.-J.; Wu, M.-F.; Chen, C.-T.; Song, Y.-H.; Chi, Y.; Ho, M.-H.; Hsu, S.-F.; Chen, C.-H. New Dopant and Host Materials for Blue-Light-Emitting Phosphorescent Organic Electroluminescent Devices. *Adv. Mater.* **2005**, *17*, 285–289.
- (16) Tsai, M.-H.; Lin, H.-W.; Su, H.-C.; Ke, T.-H.; Wu, C.; Fang, F.-C.; Liao, Y.-L.; Wong, K.-T.; Wu, C.-I. Highly Efficient Organic Blue Electrophosphorescent Devices Based on 3,6-Bis(triphenylsilyl)-carbazole as the Host Material. *Adv. Mater.* **2006**, *18*, 1216–1220.
- (17) Shih, P.-I.; Chien, C.-H.; Chuang, C.-Y.; Shu, C.-F.; Yang, C.-H.; Chen, J.-H.; Chi, Y. Novel Host Material for Highly Efficient Blue Phosphorescent OLEDs. *J. Mater. Chem.* **2007**, *17*, 1692–1698.
- (18) Hsu, F.-M.; Chien, C.-H.; Shu, C.-F.; Lai, C.-H.; Hsieh, C.-C.; Wang, K.-W.; Chou, P.-T. A Bipolar Host Material Containing Triphenylamine and Diphenylphosphoryl-Substituted Fluorene Units for Highly Efficient Blue Electrophosphorescence. *Adv. Funct. Mater.* **2009**, *19*, 2834–2843.
- (19) Tao, Y.; Gong, S.; Wang, Q.; Zhong, C.; Yang, C.; Qin, J.; Ma, D. Morphologically and Electrochemically Stable Bipolar Host for Efficient Green Electrophosphorescence. *Phys. Chem. Chem. Phys.* **2010**, *12*, 2438–2442.
- (20) Shih, P. I.; Chiang, C. L.; Dixit, A. K.; Chen, C. K.; Yuan, M. C.; Lee, R. Y.; Chen, C.-T.; Diau, E. W. -G.; Shu, C.-F. Novel Carbazole/Fluorene Hybrids: Host Materials for Blue Phosphorescent OLEDs. *Org. Lett.* **2006**, *13*, 2799–2802.
- (21) Zhang, T.; Liang, Y.; Cheng, J.; Li, J. A CBP Derivative as Bipolar Host for Performance Enhancement in Phosphorescent Organic Light-Emitting Diodes. *J. Mater. Chem. C* **2013**, *1*, 757–764.
- (22) Moorthy, J. N.; Natarajan, P.; Venkatakrishnan, P.; Huang, D.-F.; Chow, T. J. Steric Inhibition of π -Stacking: 1,3,6,8-Tetraarylpyrenes as Efficient Blue Emitters in Organic Light Emitting Diodes (OLEDs). *Org. Lett.* **2007**, *9*, 5215–5218.
- (23) Moorthy, J. N.; Venkatakrishnan, P.; Huang, D.-F.; Chow, T. J. Blue Light-Emitting and Hole-Transporting Amorphous Molecular Materials Based on Diarylamino-biphenyl-Functionalized Bimesitylenes. *Chem. Commun.* **2008**, 2146–2148.
- (24) Moorthy, J. N.; Venkatakrishnan, P.; Natarajan, P.; Huang, D.-F.; Chow, T. J. De Novo Design for Functional Amorphous Materials: Synthesis and Thermal and Light-Emitting Properties of Twisted Anthracene-Functionalized Bimesitylenes. *J. Am. Chem. Soc.* **2008**, *130*, 17320–17333.
- (25) Moorthy, J. N.; Venkatakrishnan, P.; Natarajan, P.; Lin, Z.; Chow, T. J. Nondoped Pure-Blue OLEDs Based on Amorphous Phenylenevinylene-Functionalized Twisted Bimesitylenes. *J. Org. Chem.* **2010**, *75*, 2599–2609.
- (26) Venkatakrishnan, P.; Natarajan, P.; Moorthy, J. N.; Lin, Z.; Chow, T. J. Twisted Bimesitylene-Based Oxadiazoles as Novel Host Materials for Phosphorescent OLEDs. *Tetrahedron* **2012**, *68*, 7502–7508.
- (27) Rúnarsson, O. V.; Artacho, J.; Wärnmark, K. The 125th Anniversary of the Tröger's Base Molecule: Synthesis and Applications of Tröger's Base Analogues. *Eur. J. Org. Chem.* **2012**, 7015–7041.
- (28) For our recent studies on bifunctional organic materials for OLEDs based on Tröger's Base, see: Neogi, I.; Jhulki, S.; Ghosh, A.; Chow, T. J.; Moorthy, J. N. Bifunctional Organic Materials for OLEDs Based on Tröger's Base: Subtle Structural Changes and Significant Differences in Electroluminescence. *Org. Electron.* **2014**, *15*, 3766–3772.
- (29) Brunner, K.; Dijken, A. V.; Borner, H.; Bastiaansen, J. J. A. M.; Kigger, N. M. M.; Langeveld, B. M. W. Carbazole Compounds as Host Materials for Triplet Emitters in Organic Light-Emitting Diodes: Tuning the HOMO Level without Influencing the Triplet Energy in Small Molecules. *J. Am. Chem. Soc.* **2004**, *126*, 6035–6042.
- (30) Tsai, M.-H.; Lin, H.-W.; Su, H.-C.; Ke, T.-H.; Wu, C.-C.; Fang, F.-C.; Liao, Y.-L.; Wong, K.-T.; Wu, C.-I. Highly Efficient Organic Blue Electrophosphorescent Devices Based on 3,6-Bis(triphenylsilyl)-carbazole as the Host Material. *Adv. Mater.* **2006**, *18*, 1216–1220.
- (31) Gao, Z. Q.; Luo, M.; Sun, X. H.; Tam, H. L.; Wong, M. S.; Mi, B. X.; Xia, P. F.; Cheah, K. W.; Chen, C. H. New Host Containing Bipolar Carrier Transport Moiety for High-Efficiency Electrophosphorescence at Low Voltages. *Adv. Mater.* **2009**, *21*, 688–692.
- (32) Hsu, F.-M.; Chien, C.-H.; Shih, P.-I.; Shu, C.-F. Phosphine-Oxide-Containing Bipolar Host Material for Blue Electrophosphorescent Devices. *Chem. Mater.* **2009**, *21*, 1017–1022.

(33) Huang, H.; Fu, Q.; Pan, B.; Zhuang, S.; Wang, L.; Chen, J.; Ma, D.; Yang, C. Butterfly-Shaped Tetrasubstituted Carbazole Derivatives as a New Class of Hosts for Highly Efficient Solution-Processable Green Phosphorescent Organic Light-Emitting Diodes. *Org. Lett.* **2012**, *18*, 4786–4789.

(34) Huang, H.; Wang, Y.; Pan, B.; Yang, X.; Wang, L.; Chen, J.; Ma, D.; Yang, C. Simple Bipolar Hosts with High Glass Transition Temperatures Based on 1,8-Disubstituted Carbazole for Efficient Blue and Green Electrophosphorescent Devices with Ideal Turn-on Voltage. *Chem.—Eur. J.* **2013**, *19*, 1828–1834.

(35) Xiao, L.; Chen, Z.; Qu, B.; Luo, J.; Kong, S.; Gong, Q.; Kido, J. Recent Progresses on Materials for Electrophosphorescent Organic Light-Emitting Devices. *Adv. Mater.* **2011**, *23*, 926–952.

(36) Jensen, J.; Wärnmark, K. Synthesis of Halogen Substituted Analogues of Tröger's Base. *Synthesis* **2001**, *12*, 1873–1877.

(37) Jensen, J.; Strozyk, M.; Wärnmark, K. Influence of Scale, Stoichiometry and Temperature on the Synthesis of 2,8-dihalo Analogues of Tröger's Base from the Corresponding Anilines and Paraformaldehyde. *J. Heterocycl. Chem.* **2003**, *40*, 373–375.

(38) Hansson, A.; Jensen, J.; Wendt, O. F.; Wärnmark, K. Synthesis of Dihalo-Substituted Analogues of Tröger's Base from *ortho*- and *meta*-Substituted Anilines. *Eur. J. Org. Chem.* **2003**, 3179–3188.

(39) Lamansky, S.; Djurovich, P.; Murphy, D.; Abdel-Razzaq, F.; Kwong, R.; Tsyba, I.; Bortz, M.; Mui, B.; Bau, R.; Thompson, M. E. Synthesis and Characterization of Phosphorescent Cyclometalated Iridium Complexes. *Inorg. Chem.* **2001**, *40*, 1704–1711.

(40) Holmes, R. J.; Forrest, S. R.; Tung, Y. J.; Kwong, R. C.; Brown, J. J.; Garon, S.; Thompson, M. E. Blue Organic Electrophosphorescence Using Exothermic Host-Guest Energy Transfer. *Appl. Phys. Lett.* **2003**, *82*, 2422–2424.

(41) Diouf, B.; Jeon, W. S.; Pode, R.; Kwon, J. H. Efficiency Control in Iridium Complex-Based Phosphorescent Light-Emitting Diodes. *Adv. Mater. Sci. Eng.* **2012**, DOI: 10.1155/2012/794674.

(42) Salert, B. C. D.; Wedel, A.; Grubert, L.; Eberle, T.; Anémian, R.; Krueger, H. Polystyrene Backbone Polymers Consisting of Alkyl-Substituted Triazine Side Groups for Phosphorescent OLEDs. *Adv. Mater. Sci. Eng.* **2012**, DOI: 10.1155/2012/385178.